Article
Beitr. Phys. Atmosph., August 1993, p. 239–252
0005-8173/93/3 0239–14 $ 3.00/0
Vol. 66, No.3 239

Orographic Forcing in ECHAM

by R. SAUSEN[1], R. VOSS[2] and M. PONATER[1]

[1]Deutsche Forschungsanstalt für Luft- und Raumfahrt, Institut für Physik der Atmosphäre, Oberpfaffenhofen, 82230 Weßling, Germany
[2]Meteorologisches Institut der Universität Hamburg, Bundesstraße 55, 20146 Hamburg, Germany

(Manuscript received August 14, 1992; accepted September 14, 1993)

Abstract

In the current generation of general circulation models the orographic height is prescribed according to the horizontal resolution, using either grid-box averaged values, or including an envelope increment to capture the actual barrier effect of the mountain ranges in the real world. Generally, a gravity wave drag (GWD) parameterization is also included to account for the decelerating influence of gravity wave breaking on the upper level large-scale flow.

To study in a systematic way the consequences of various possible approaches for the model climate, a set of experiments with the ECHAM general circulation model in T21 horizontal resolution was performed. The results indicate that the use of the envelope orography as well as the use of the ECMWF GWD scheme has a distinctly negative impact on the simulation of Northern Hemisphere winter circulation. The most realistic simulation is yielded, if the model is run with mean orography and without GWD parameterization. It is evident from the experiments that the treatment of the orographic effects in high resolution models must not be applied to climate models without careful adjustment to the actual (low) horizontal resolution.

Zusammenfassung

Orographischer Antrieb in ECHAM

In der heutigen Generation von Zirkulationsmodellen wird die Höhe der Orographie entsprechend der horizontalen Auflösung beschrieben. Dazu wird entweder das beobachtete Orographiefeld über die jeweiligen Gitterboxen gemittelt („Mean"-Orographie) oder man berücksichtigt zusätzlich eine „Envelope"-Erhöhung, die den Barriereneffekt der Gebirgsregionen besser berücksichtigen soll. Eine „Gravity-Wave-Drag"-Parameterisierung (GWD) wird ebenfalls berücksichtigt, um den bremsenden Einfluß von brechenden Schwerewellen in den höheren Niveaus der großräumigen Strömung zu beschreiben.

Um die Konsequenzen verschiedener möglicher Ansätze auf das Modellklima systematisch zu studieren, wurde eine Serie von Experimenten mit dem Zirkulationsmodell ECHAM in T21 Auflösung gemacht. Die Ergebnisse zeigen, daß die Benutzung der „Envelope"-Orographie ebenso wie die Verwendung des ECMWF GWD-Schemas einen eindeutig negativen Einfluß auf die Simulation der nordhemisphärischen Winterzirkulation hat. Die beste Simulation wird erreicht, wenn das Modell mit „Mean"-Orographie und ohne GWD-Parameterisierung betrieben wird. Aus den Experimenten wird deutlich, daß die Behandlung der orographischen Effekte in hoch aufgelösten Modellen nicht ohne sorgfältige Anpassung auf grobauflösende Klimamodelle übertragen werden darf.

1 Introduction

Orography has a large impact on the atmosphere on all scales from global to microscale. Beside the land-sea contrast it is the strongest force introducing a zonal asymmetry into the atmospheric time mean flow. The daily mean of the near surface temperature (2 m) is strongly influenced by the orographic height of the location under consideration. Lee waves can be triggered, if the large-scale flow crosses a mountain. In the Northern Hemisphere, the orography determines the position of the troughs and ridges of the quasi-stationary planetary waves. Another effect of the orography is the retardation

of fronts (e.g. Egger and Hoinka, 1992). This list of orographic influences could easily be extended. Obviously the major orographic effects have to be included in any general circulation model. Some of these impacts can be resolved by the scale of the model; others have to be parameterized, where the way of parameterization depends on the resolution of the model.

In general circulation models, orography has a direct and an indirect impact on the simulated flow. Directly, orography enters the models via the lower boundary conditions or (in the case of terrain following coordinates) by the presence of additional terms in the primitive equations. Indirectly, the orography influences the model climate by parameterizations of subgrid-scale processes, such as orographically excited gravity waves. In the real atmosphere, these waves can propagate in the vertical and may reach considerable altitudes, depending on the atmospheric stability and the vertical wind shear. Bretherton (1969), Lilly (1972) and others suggested that gravity wave activity may provide an important forcing on the large-scale flow in regions of wave momentum flux divergence (e.g. in regions, where the waves are dissipated or absorbed). This phenomenon is called **G**ravity **W**ave **D**rag (GWD).

As internal gravity waves have a typical length of the order of ten kilometres, they are not represented in a model with a resolution of some hundred kilometres. The necessity to limit the GCM climate drift in extended range forecasts and climate integrations lead to the development of GWD parameterization schemes to account for the drag effect on the large scale flow. Such schemes were shown to reduce the systematic errors of the time-averaged flow both in high-resolution (T42 and higher) forecasts with the ECMWF[1] model (Shutts, 1985; Palmer et al., 1986; Miller et al., 1989) and in long-range simulations at low resolution with the Canadian Climate Centre GCM (Boer et al., 1984; McFarlane, 1987).

The direct impact of orography on the atmospheric flow is induced by the barrier effect of the large-scale elevations. A mountain can induce, for example, broad horizontal excursions of the wind or orographic rainfalls on the windward slopes. The height of a mountain determines the fractions of air passing around or over this mountain, respectively. However, if an atmospheric model with a resolution of some hundred kilometres is used, the mean height averaged over a grid box will underestimate the actual height of most mountain ranges. As a consequence the wind tries to go more frequently over the mountains than observed (Jarraud et al., 1985). In order to counteract this effect an enhanced orography – a so-called envelope orography – has been developed (Wallace et al., 1983).

In the present study we use the general circulation model ECHAM (**EC**MWF-model in **HAM**BURG) to study the effects mentioned above. ECHAM was developed as a sophisticated tool for climate simulations. It is based on the spectral numerical weather forecast model of ECMWF (Simmons et al., 1989), but many parameterizations schemes of physical processes have been exchanged in order to make the model more appropriate for climate applications (Roeckner et al., 1992). The first operational version (ECHAM-1) used a T21 horizontal resolution with 19 vertical levels (e.g. Cubasch et al., 1992). Due to the favourable experience in previous studies, the orographic effects described above were represented by using an envelope orography and the ECMWF parameterization scheme of the GWD (Palmer et al., 1986). The model was integrated over 20 annual cycles in the control mode, i.e. with prescribed climatological sea surface temperature. A number of systematic errors within this integration suggest an inadequate representation of orographic effects.

Figure 1 shows the time-averaged mean sea level pressure for January. The model results (a) show an erroneous high pressure over the Arctic basin relative to observations (b). The Icelandic low is badly represented both in position and strength. One might speculate, that these defects are caused by an excessively decelerating effect of the orography in the North American-Greenland area. Further indications for this hypothesis can be found in the zonal mean of the zonal wind for January (Figure 2). ECHAM-1 underestimates the polar night jet in the stratosphere of the Northern Hemisphere in comparison to the ECMWF analyses. The distribution of the zonal mean temperature shows a strong warm bias at these levels. As the GWD is particularly effective in the wintertime Arctic stratosphere (Rind et al., 1988), it might be assumed that the parameterization scheme of the GWD contributes to this model defect.

While there is a lot of heuristic argument to blame the use of envelope orography and GWD to produce the error patterns mentioned above, this conclusion would contradict some of the previous findings (Miller et al., 1989; McFarlane, 1987). In order to provide convincing evidence that the defects are caused by an inadequate orographic

[1] European Centre for Medium Range Weather Forecasts

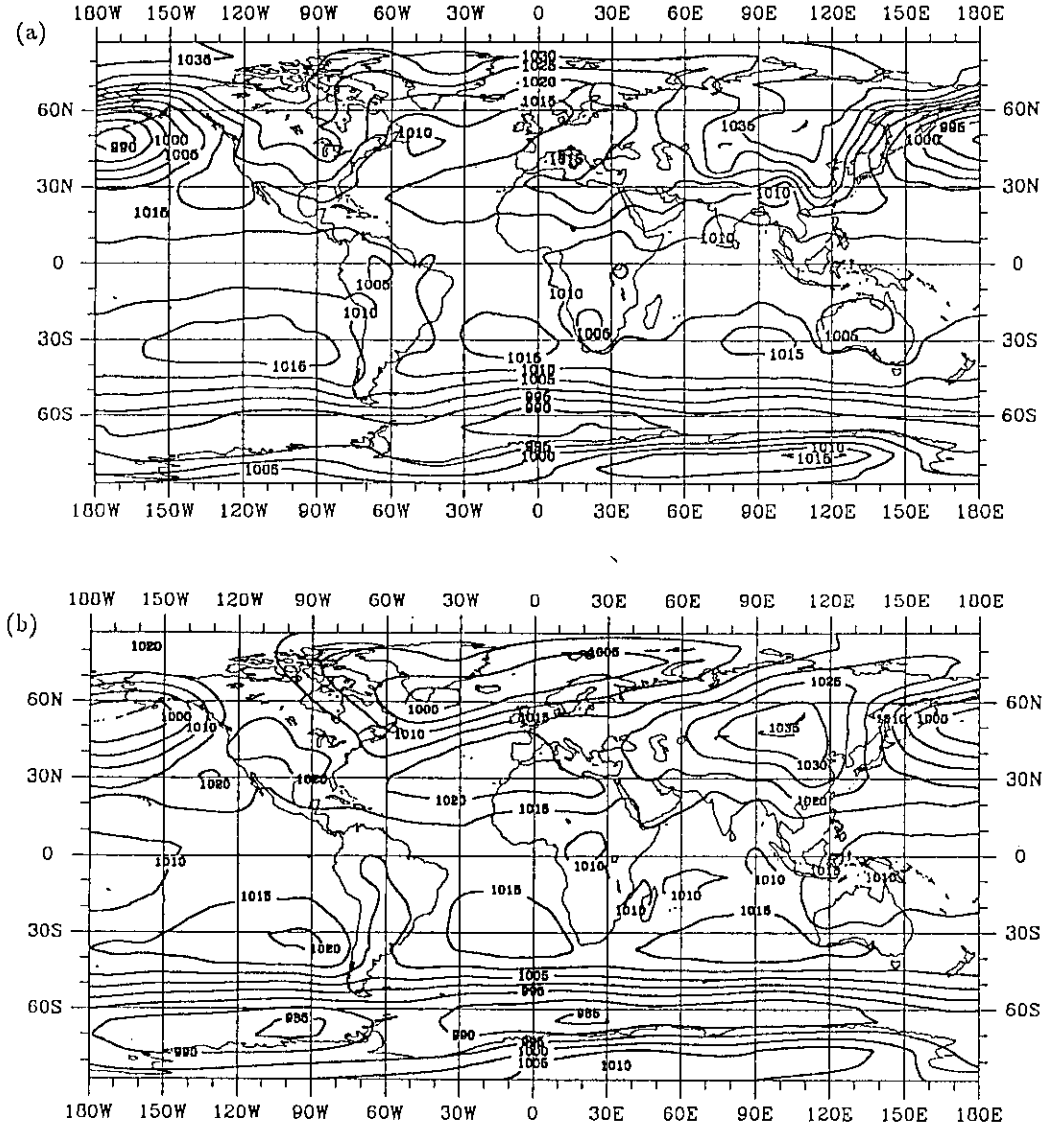

Figure 1 Mean sea level pressure [hPa] of January for: a) ECHAM-1 (mean of 20 years); b) ECMWF level IIIb analysis (mean of 1979–1986).

forcing a more detailed and systematic approach is required. To this end three pairs of perpetual January integrations (i.e. with diurnal but without seasonal cycle of insolation) were performed, each pair consisting of one run with and another run without the GWD parameterization. The first pair used envelope orography, the second mean orography and the third no orography. All runs were integrated over 180 days. The results of these runs will be compared in the following Sections 2 and 3. A discussion will be given in the concluding Section 4.

2 Impact of the Gravity Wave Drag Scheme

Internal gravity waves are excited by a stratified flow over irregular terrain. These waves are able to propagate vertically to great heights, and they transport momentum upward from the source regions to those levels, where the waves are dissipated or absorbed. In association with the dissipation or absorption a wave momentum flux divergence occurs

$$\left(\frac{d\mathbf{v}}{dt}\right)_{gw} = -g\frac{\partial \tau_{gw}}{\partial \eta}, \qquad (1)$$

where $\left(\frac{d\mathbf{v}}{dt}\right)_{gw}$ is the tendency of the horizontal velocity due to GWD, g is the gravity acceleration, η the vertical coordinate (bearing the dimension of pressure) and τ_{gw} is the vertical momentum flux due to gravity waves. This divergence creates a feedback on the large-scale flow. It can be parameterized on

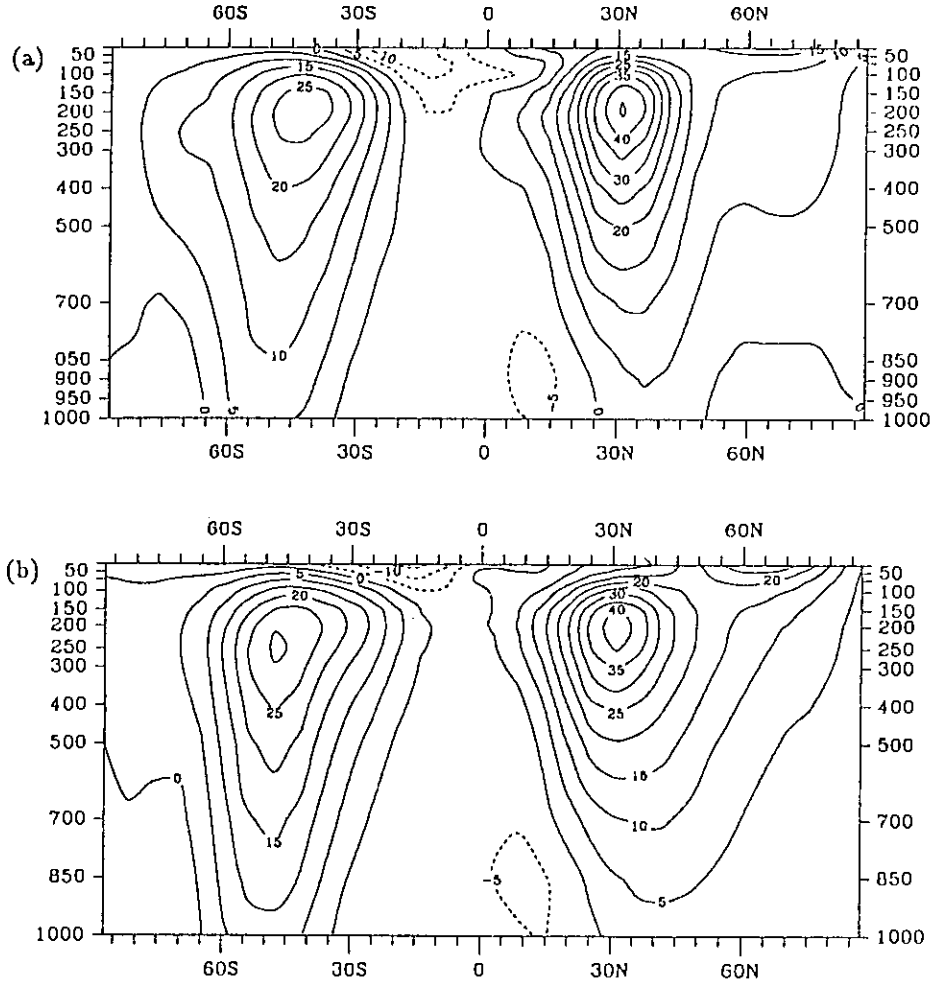

Figure 2 Zonal mean cross-section of the zonal wind [m/s] of January for: a) ECHAM-1 (mean of 20 years); b) ECMWF level IIIb analysis (mean of 1979–1986). The contour interval is 5 m/s, negative isotaches are dashed.

the basis of the two-dimensional linear theory of gravity waves (Shutts, 1985). At the lower boundary of the model (surface) the subgrid scale orography induces a vertical (gravity wave) momentum flux which is parameterized by

$$\tau_{gw}^{(s)} = \rho_S K N_S v_S |\delta h (v_S)|^2. \quad (2)$$

Here ρ_S is the density at the surface, N_S the Brunt-Vaisäla frequency, v_S the surface horizontal wind, and K is a tuning parameter. $\delta h (v_S)$ indicates the standard deviation of the subgrid scale orography in the direction of the surface wind v_S. Thus the anisotropic structure of the orography is taken into account, but for practical reasons only four main directions are considered: N-S, E-W, NW-SE, NO-SW. $\delta h (v_S)$ is calculated from a high resolution orography data set. It is prescribed independently from the model orography actually used.

The momentum flux due to the gravity waves $\tau_{gw}^{(s)}$, which is induced at the surface, is absorbed in the free atmosphere. In ECHAM, the absorption is parameterized in the same way as in the ECMWF model according to the following scheme:

Assume that $\tau_{gw}^{(\ell+1)}$ is the momentum flux entering level ℓ from the level $(\ell+1)$ below.[2] Then we calculate a hypothetical vertical displacement $|\delta z_\ell|$, which is caused by gravity waves at level ℓ, according to

$$\tau_{gw}^{(\ell+1)} = \rho_\ell K N_\ell v_\ell |\delta z_\ell|^2. \quad (3)$$

Here ρ_ℓ and N_ℓ are the density and the Brunt-Vaisäla frequency at level ℓ, v_ℓ is the projection of the wind at level ℓ onto the direction of the surface wind v_S, Using the displacement $|\delta z_\ell|$ as a measure of the wave stability, the so-called wave Richardson

[2] The top level is $\ell = 1$ and the bottom level is $\ell = 19$.

number $Ri^{(\ell)}$ – is determined

$$Ri^{(\ell)} = \frac{N_\ell^2\left(1 - \frac{N_\ell|\delta z_\ell|}{|v_\ell|}\right)}{\left(n_\ell + \frac{N_\ell|\delta z_\ell|}{|v_\ell|}\right)^2}, \quad (4)$$

where n_ℓ is the vorticity in a two-dimensional plane with the vertical coordinate η and a horizontal coordinate in direction of the surface wind v_s. If $Ri^{(\ell)} \geq Ri_{krit} = 0.25$, the gravity waves are stable and no momentum is absorbed at level ℓ. This results in

$$\tau_{gw}^{(\ell)} = \tau_{gw}^{(\ell+1)}. \quad (5)$$

If $Ri^{(\ell)} < Ri_{krit}$, a new displacement $|\delta\hat{z}_\ell|$ is determined from (4) such that the new wave Richardson number becomes $\hat{Ri}^{(\ell)} = Ri_{krit}$. Then the momentum flux at level ℓ is

$$\tau_{gw}^{(\ell)} = \rho_\ell K N_\ell v_\ell |\delta\hat{z}_\ell|^2. \quad (6)$$

The flux $|\tau_{gw}^{(\ell+1)}| - |\tau_{gw}^{(\ell)}|$ is absorbed at level ℓ. At the top of the model we use the boundary condition $\tau_{gw}^{(1)} = 0$.

The verification of the parameterized forcing field is rather difficult, as observations of the vertical wave momentum flux are not available on a global scale. However, the simulated features of the wave momentum flux τ_{gw} and the forcing by GWD $(dv/dt)_{gw}$ are consistent with local observations. Figure 3 shows for a selected gridpoint (41.5° N, 112.5° E) the model results of $\tau_{gw} = |\tau_{gw}|$ and $dv/dt = |(dv/dt)_{gw}|$ from a perpetual January run with envelope orography. The lower troposphere and the lower stratosphere are regions of wave breaking (i.e. of momentum flux divergence) in accordance with observations (cf. Lilly and Kennedy, 1973). However, depending on local stability and advection also gridpoints can be found with only one maximum or even without any distinct maximum of wave momentum flux divergence.

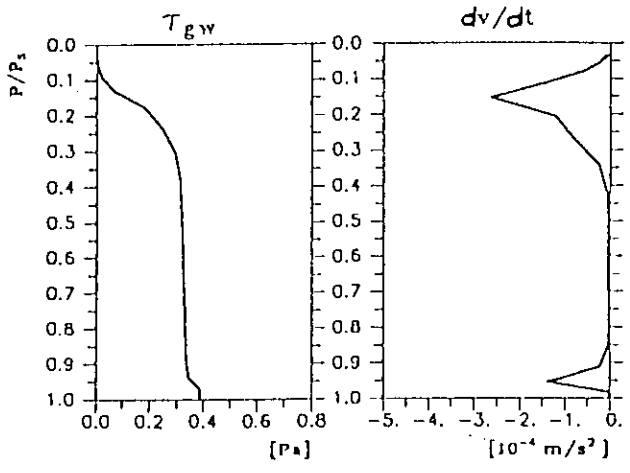

Figure 3 Vertical profiles of the wave momentum flux τ_{gw} (left panel) and the forcing by GWD $(dv/dt)_{gw}$ (right panel) for the grid point 41.5° NB, 112.5° E of an experiment with envelope orography. Mean of days 91–720 of a perpetual January run. At this grid point the standard deviation of the orography δh is 250 m.

For a more global illustration Figures 4 and 5 show the horizontal distributions of the forcing by GWD $(dv/dt)_{gw}$ for the model levels 3 (lower stratosphere) and 16 (lower troposphere).[3] In the lower troposphere the GWD induced by the Himalayas, the East Siberian mountains, the SE-Asian mountains, the Rocky Mountains, the Andes, the East African mountains, Greenland and the edge of Antarctica can be identified. The stratospheric GWD exhibits its highest values in the mid-latitudes of the Northern Hemisphere, especially over Mongolia and Greenland. South of 25 °N the GWD is rather weak. In the tropics and summer extra-tropics the vertical structure of the atmosphere differs from the winter extra-tropics, and the momentum propagating upward is absorbed already at lower altitudes. Furthermore, due to smaller surface wind less mountain effect is generated in these regions. The middle and upper troposphere exhibits no significant GWD (not shown) as already suggested by Figure 3.

We will now study the effect of GWD action on several model variables by comparing results from the runs with envelope orography. Figure 6 shows the time-averaged zonal mean of the zonal wind for two experiments with (a) and without (b) the parameterization of the GWD. It is evident that the main differences between both experiments occur at lower stratospheric levels of the northern middle and high latitudes. Though the internal variance is strongest here, the differences are significant in a statistical sense. The zonal wind maxima in the experiment with GWD are weaker, particularly the polar night jet core exhibits a deceleration of more than 10 m/s. The same significant difference pattern is found in experiments with mean orography and even without orography (not shown). (For the run

[3] As ECHAM uses hybrid σ-p coordinates, the actual heights of the model levels depend on the surface pressure.

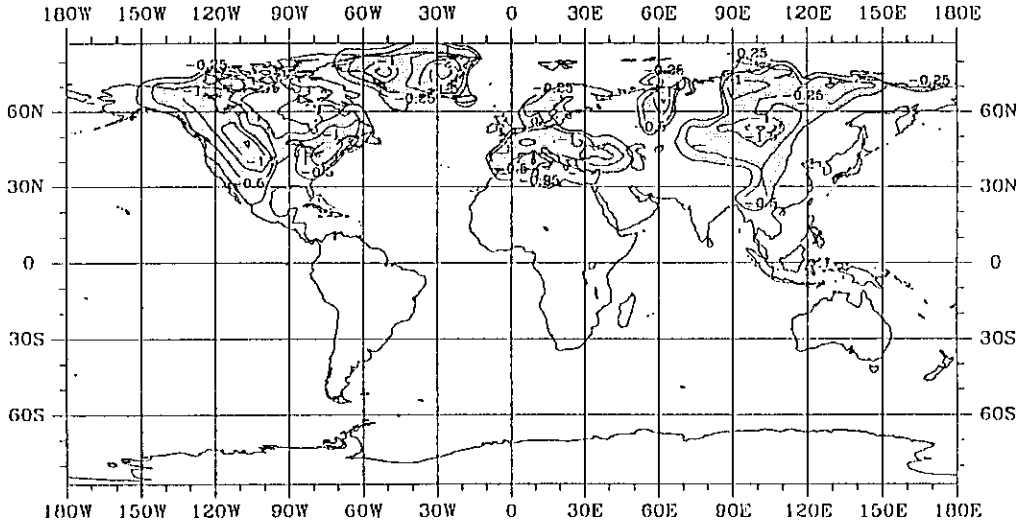

Figure 4 $(dv/dt)_{gw}$ at the model level 3 (lower stratosphere) for an experiment with envelope orography. Isolines for $[0.25, 0.5, 1., 1.5, 2., 2.5, 3., 3.5, 4] \cdot 10^{-4}$ m/s^2. Areas with values larger than $0.25 \cdot 10^{-4}$ m/s^2 are shaded.

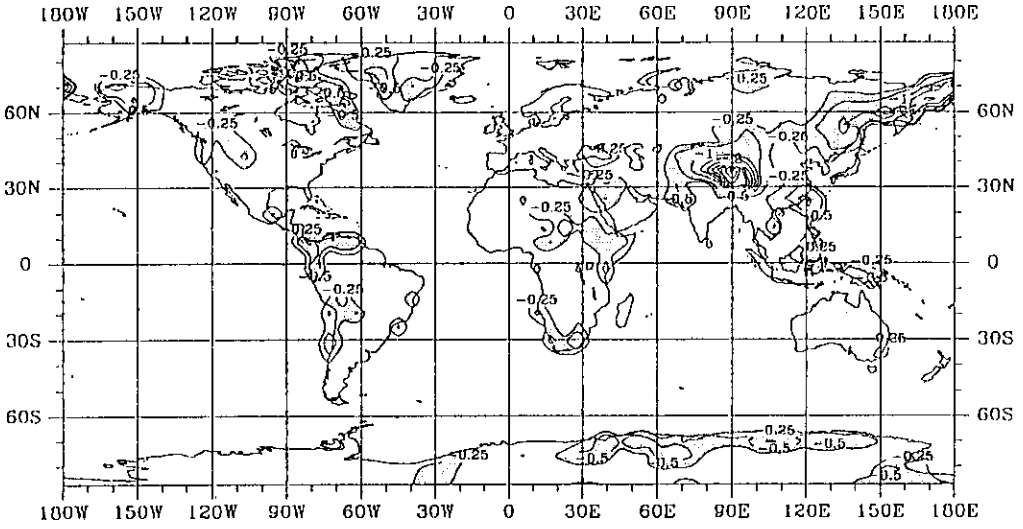

Figure 5 As Figure 4, but for the model level 16 (lower troposphere).

with GWD but without orography, the surface elevation was set to zero while the standard deviation of the real orography was not removed in the GWD parameterization. This artifical sensitivity experiment allows the simulation of the effect of GWD even in a world without orography.) The underestimation of the polar night jet in ECHAM-1 (Figure 2) can clearly be attributed to the influence of the GWD parameterization.

Figure 7 shows the zonal mean temperature of the experiments with (a) and without (b) GWD and the ECMWF observations (c). Again the most obvious differences are found in the upper levels of northern middle and high latitudes. With GWD the observed temperature distribution is badly simulated, exhibiting a strong warm bias poleward of 60 °N. The structure of the temperature field is improved in the experiment without GWD, but now the observed values are underestimated. GWD increases the temperature by more than 10 K in certain regions. Also in the upper levels of the Southern Hemisphere systematic temperature errors are found, but they are similar in both experiments. As this is confirmed by the analogous runs with mean and without orography, Southern Hemispheric systematic errors seem to be largely independent from the GWD parameterization.

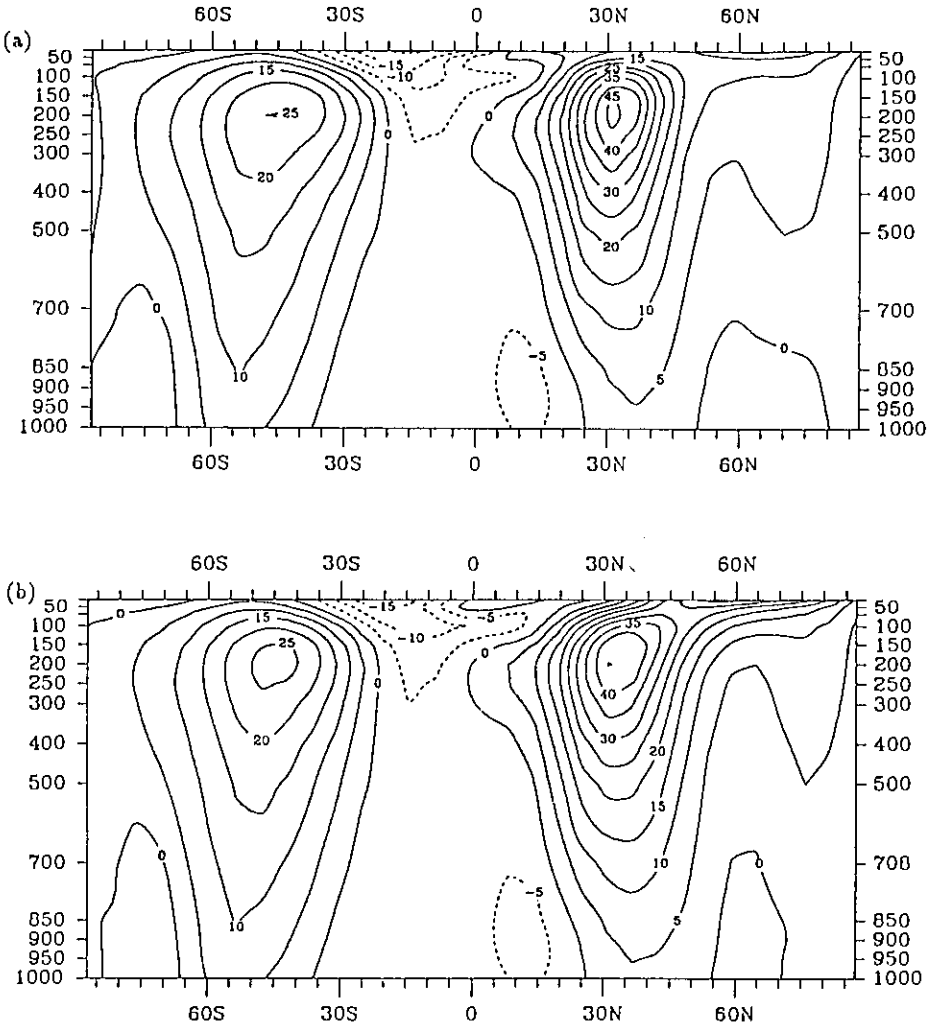

Figure 6 Zonal mean values of the zonal wind [m/s] for perpetual January simulations with (a) and without (b) GWD (means of days 61–180). The contour interval is 5 m/s, negative isotaches are dashed.

The time-averaged pressure field at mean sea level for the experiments with and without GWD (in both cases with envelope orography) exhibits distinct differences mainly in the Arctic region (Figure 8). GWD induces a significant and unfavourable rise of pressure. Figure 8a closely resembles the erroneous high over the same region as in the control integration with ECHAM-1 (Figure 1a). A similar rise of pressure in the Arctic region is found in the corresponding pair of experiments using the mean orography (Figure 9).

3 Impact of the Specification of Orography

The orography directly enters the model equations of ECHAM via the lower boundary condition, which is used in the spectral domain of the model. The conventional "mean orography" is determined in a two-step procedure: First, the observed orography (U.S. Navy dataset with (1/6)° resolution) is averaged over each box of T21 Gaussian grid (grid size approx. 5.6°). The resulting elevations are then transformed to the model's spectral domain and truncated to the model resolution (here T21, which corresponds to a homogeneously isotropic resolution of approx. 8.6° for the dynamics of the model). Figure 10a shows the mean orography which has been transformed back in the grid point domain after spectral adjustment. Only the very large scale structures can be reproduced, for example Greenland, the Rocky Mountains, the Himalayas and Antarctica. Due to the Gibbs phenomenon also spurious mountains and valleys exist over the oceans.

As mentioned in the introduction the envelope orography has been developed in order to enhance the barrier effect of the mountain ranges (Wallace et al., 1983; Tibaldi, 1986). The envelope orography

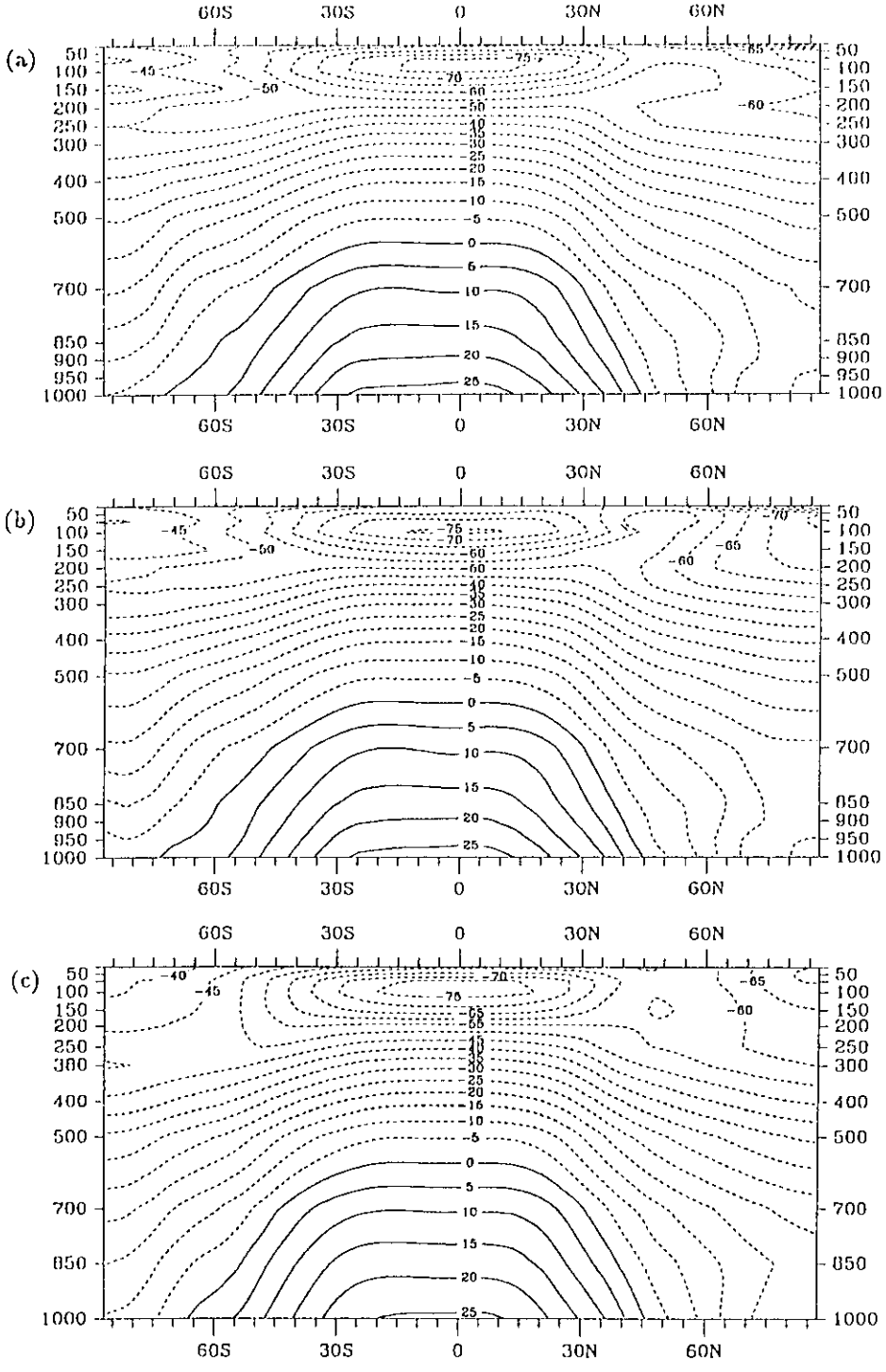

Figure 7 Zonal mean temperature [°C] of experiments with GWD (a), without GWD (b) (means of days 61–180) and ECMWF level IIIb analysis for January (c) (means of 1979–1986). The contour interval is 5 °C, negative isothermes are dashed.

is created by adding the standard deviation of the observed subgrid-scale orography to the mean grid-point values. Adding the envelope increment increases the maximum height of mountain ranges and the area covered by mountain terrain (Figure 10b).

Figure 11 shows three selected profiles of mountain ranges. The thin lines represent the U.S. Navy data (solid: mean heights, dashed: mean heights plus one standard deviation). The upper thick curve represents the envelope orography and the lower curve the mean orography. The profile of the Rocky

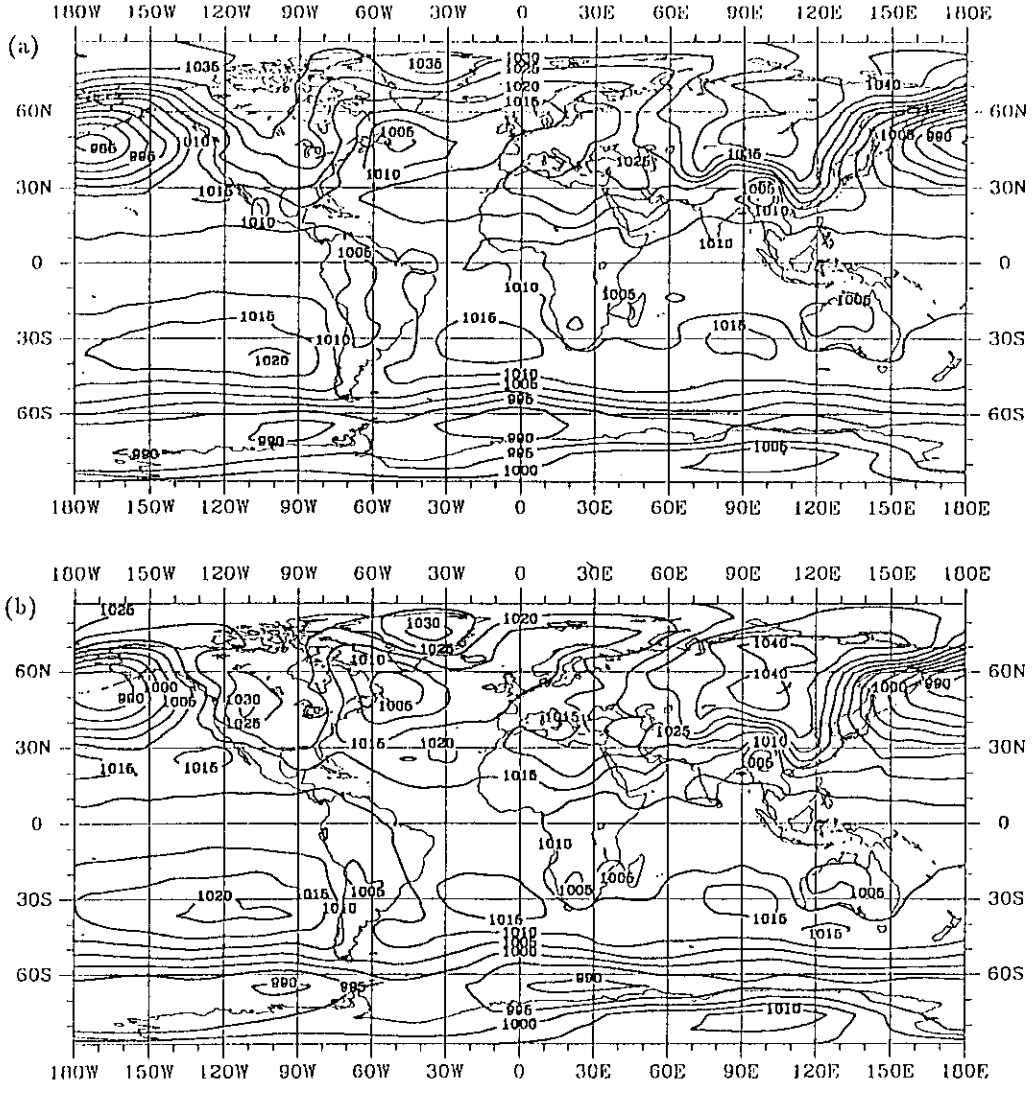

Figure 8 Mean sea level pressure [hPa] for experiments with envelope orography with (a) and without GWD (b). Mean of days 61–180.

Mountains (Figure 11a) shows that the envelope orography tends to follow the top of the mountains whereas the mean orography follows the mean heights. Both model orographies represent roughly the shape of the mountain range. The shape of the Alps (Figure 11b) is almost ignored in either case. The characteristic barrier in north south direction is not reproduced. The steep coasts of Greenland are insufficiently represented as a consequence of the low model resolution (Figure 11c). The slope is too weak. In both cases the elevation of Greenland extends far beyond the real coastline. The envelope orography shows a realistic maximum height over Greenland, but the slopes extend even farther away from the actual mountain location than in the case with mean orography. However, this bad representation of Greenland is a particular problem of the T21 resolution, which is nearly solved by increasing the resolution to T42.

The differences between simulations with envelope and mean orography show up mainly in the horizontal structure of the flow field. As an example, we discuss again the mean sea level pressure for the experiments with mean orography, both with and without GWD (Figure 9). They can be compared with the respective results with envelope orography (Figure 8). Here we have to note that this intercomparison should be performed rather with respect to structure differences than to absolute values, as the runs with envelope orography and with mean orography have different global averages of the mean sea level pressure. In the sensitivity experiments discussed above the global average of the surface pressure is identical, i.e. the total mass is

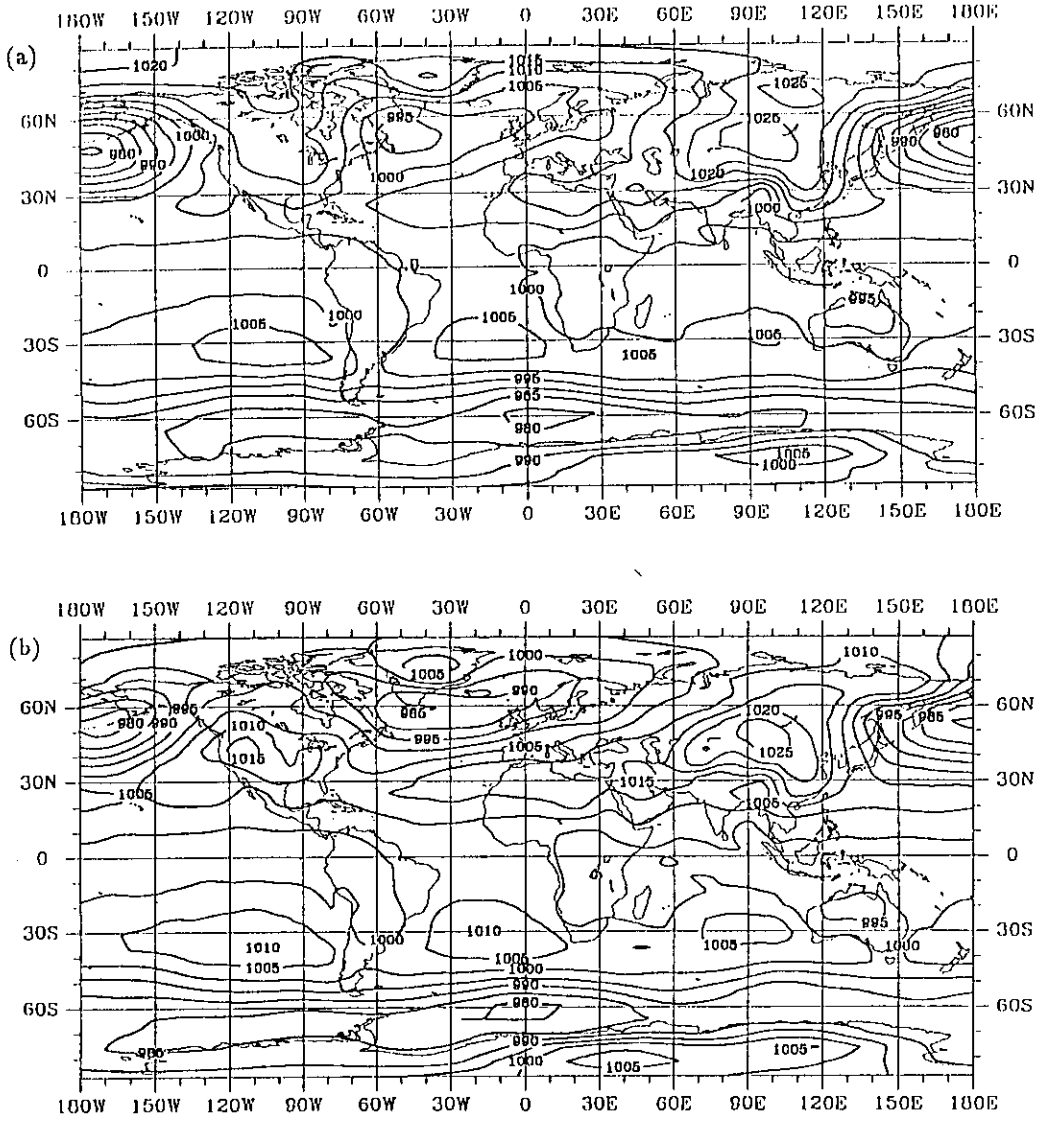

Figure 9 Mean sea level pressure [hPa] for experiments with mean orography with (a) and without GWD (b). Mean of days 61–180.

identical in these runs. In general, the spectrally adapted envelope orography is higher than the spectrally adapted mean orography. Consequently, the extrapolation to the mean sea level will give different results. If we assume an identical temperature field (vertically as function of pressure) and an identical surface pressure field, the global average of the mean sea level pressure will be higher in the case of the envelope orography than in the case of mean orography.

Generally, the erroneous Arctic pressure high is reduced by use of the mean orography, but a substantial improvement is reached only in the absence of GWD (Figure 9b). The run with mean orography and without GWD clearly offers the most realistic simulation. Only in this case the Rocky Mountains are crossed by southwesterly winds at 50° N as observed, while the other runs simulate a flow mainly parallel to this mountain ridge. Moreover, Figure 9b shows a reasonable representation of the climatological Icelandic low with westerlies blowing towards Northern Europe, a feature hardly present in the other experiments. With respect to systematic errors in other areas the four runs in Figures 8 and 9 do not differ significantly. In particular the Southern Hemisphere extratropical westerlies are too weak, and the subpolar low around Antarctica is not deep enough relative to observations (Figure 1b).

4 Discussion

Six sensitivity experiments were performed to study the impact of a GWD parameterization and the use of an envelope orography on the January climate simulated by the ECHAM/T21 GCM.

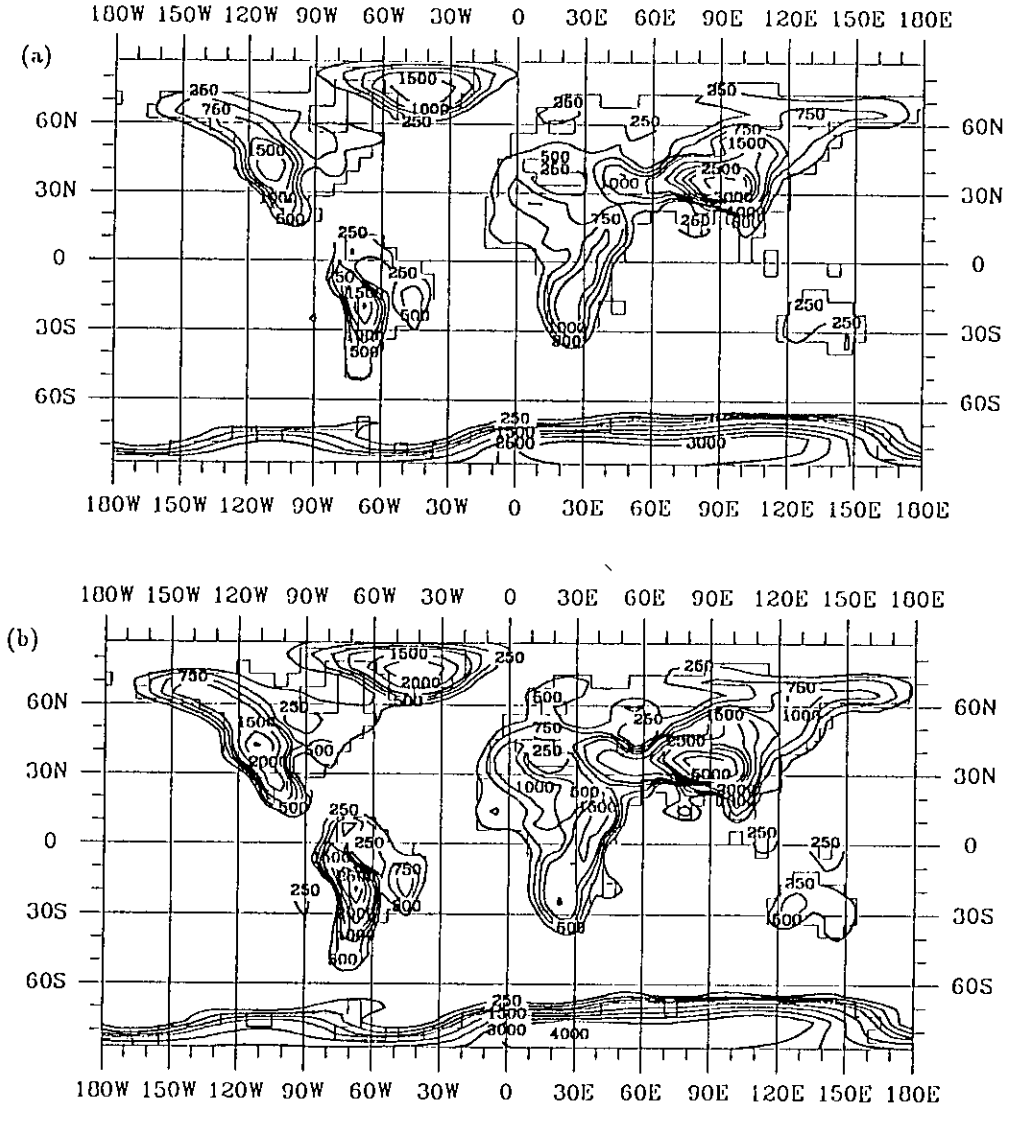

Figure 10 The spectrally adapted mean (a) and envelope (b) orographies for T21 resolution. Isolines for 250, 500, 750, 1000, 1500, 2000, 2500, 3000, 4000, 5000 m.

The modification induced by the GWD scheme are consistent with local observations (e.g. Lilly and Kennedy, 1973). A warming and a weakening of the zonal flow in the stratosphere of northern middle and high latitudes is found. These features are desired for models with an overestimation of mid-latitude zonal winds, particularly models of higher resolution (Palmer et al., 1986; Laursen and Eliasen, 1989). However, the climate of ECHAM with T21 horizontal resolution is substantially deteriorated. The pressure over the Arctic basin becomes excessively high and the Icelandic low is shifted to the southwest. If the GWD parameterization is switched off, the results are closer to the observations, particularly in the presence of the mean orography.

The introduction of envelope orography helps to alleviate systematic errors in models of resolution higher than T21 (Tibaldi, 1986). For a T21 model the representation of the shape of mountain ranges is just as bad with envelope orography than with mean orography. Using the envelope orography the favourable effect arising from an omission of the GWD scheme to the T21 results is partly prohibited.

The systematic perpetual January studies clearly suggest that an ECHAM/T21 model version with mean orography and without a GWD parameterization is likely to simulate the three-dimensional time mean fields closest to the observations. This indication was confirmed by a 20-year annual cycle integration with that version (now with corrected mass of the atmosphere). Again the mean sea level pressure field is used to demonstrate the overall effect (Figure 12). All favourable features known from Figure 9b are also evident in Figure 12 (to be

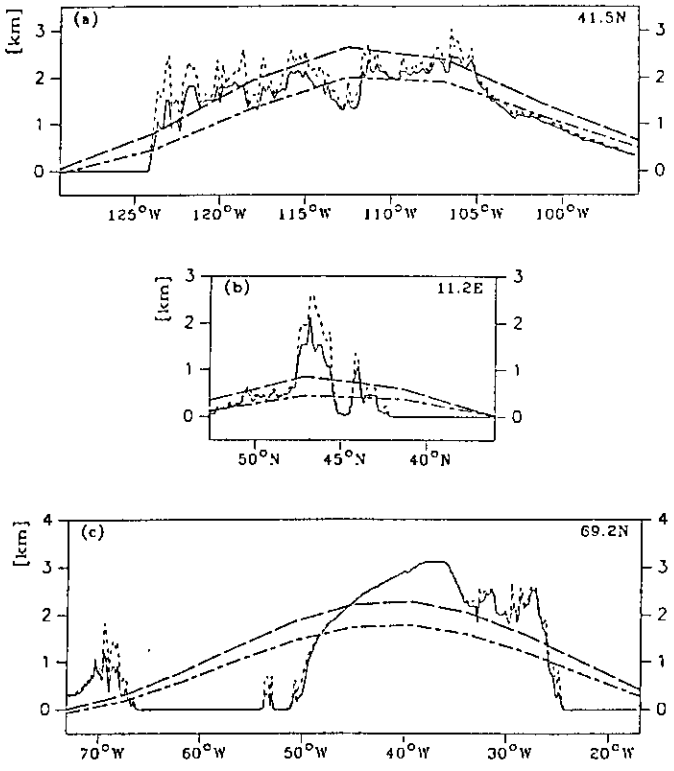

Figure 11 Cross-sections through mountain ranges showing envelope orography (upper thick curve), mean orography (lower thick curve), mean height for the U.S. Navy dataset (thin solid curve) and mean height plus standard deviation for the U.S. Navy dataset (thin dashed curve). (a) the Rocky Mountains, (b) the Alps, (c) Greenland.

compared with Figure 1). It should be added that also the large-scale variability of the atmosphere is simulated more realistically as a consequence of the improvements of the time-mean fields (Tibaldi et al., 1990; Ponater and König, 1991). All results reported above lead to a change of the operational version of ECHAM from ECHAM-1 (Figure 1) to ECHAM-2 (Figure 12).

It may seem surprising that the version (ECHAM-2) which neglects the observed effect of GWD and which has a less reasonable representation of the mountain barrier effect simulates the climate more realistically than the version (ECHAM-1), which includes these effects. However, as already assumed by Palmer (1987), this is most probably caused by a compensation of errors: In T21 resolution the meridional eddy momentum transports, and thus the upper level forcing of the zonal flow, are underestimated. This defect can be seen for both ECHAM-1 and ECHAM-2 (Figure 13) and is particularly pronounced for the cyclonic time-scale. The underestimation of cyclone-scale momentum flux convergence is (for ECHAM-2) compensated by the absence of GWD as a frictional sink of momentum. The compensation effect occurs for Northern Hemisphere winter only, hence the weak zonal flow of Southern Hemisphere mid-latitudes is not changed in ECHAM-2 (Figure 2; see also Roeckner et al., 1992). These findings seem to be common with other low resolution general circulation models. The only one among these, where GWD was applied successfully, is the Canadian Climate Centre GCM. This model, however, is characterized by excessive westerlies, if run without GWD (McFarlane, 1987). It has been assumed (Miller et al., 1989) that this is the consequence of a particularly weak frictional coupling between the atmosphere and the earth's surface.

Considering the upper level cold bias in the experiments without GWD parameterization (Figure 7),

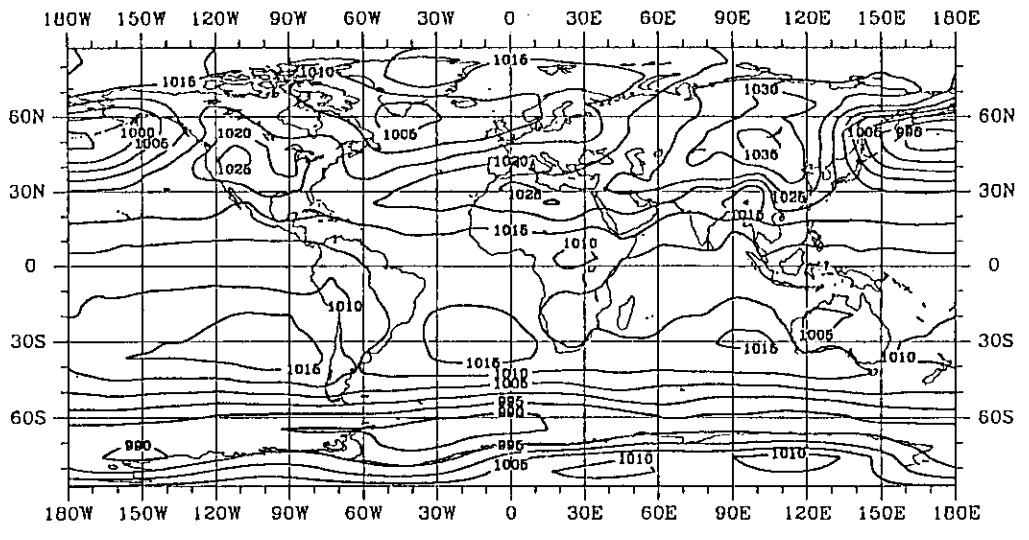

Figure 12 Mean sea level [hPa] pressure of January for ECHAM-2 (mean of 20 years).

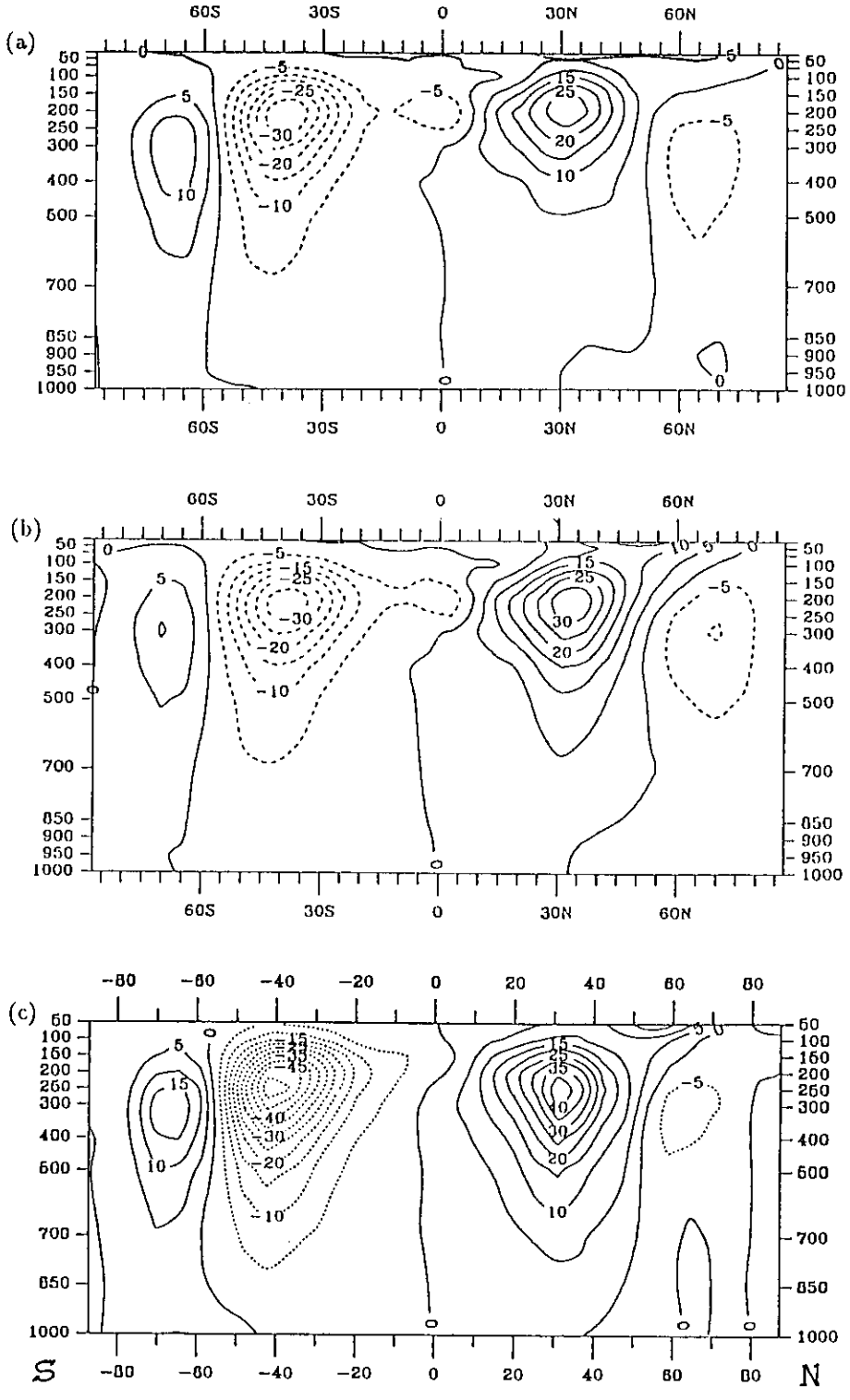

Figure 13 Zonal mean of the meridional transport by transient eddies $u'v'$ [m^2/s^2] for ECHAM-1 (a), ECHAM-2 (b) and for ECMWF level IIIb analysis (c) (mean of 1979–1986). The contour interval is 5 m^2/s^2, negative contours are dashed.

which are accompanied by excessive stratospheric westerlies, the use of the GWD parameterization for models with a horizontal resolution comparable to T21 need not be utterly rejected. However, the parameterization must act on a more moderate level and a careful adjustment of the standard GWD parameterization scheme is required.

GCMs with higher resolution generally display a reasonable representation of transient eddy momentum fluxes, even with a tendency towards overestimation. Thus they have to be run with the fully effective GWD parameterization in order to yield a realistic Northern Hemisphere winter climate. This has turned out to be true also for ECHAM at T42 horizontal resolution (Roeckner et al., 1992).

Acknowledgements

This research was supported by the Commission of the European Communities through grants EV4C-0031-D (until November 1991) and EPOC-0003-C (MB), as well as by the German Federal Ministry of Research and Technology (BMFT) through grant 07 KFT 05/6. The authors wish to thank their colleagues, esp. Günther Fischer and Erich Roeckner for many helpful and encouraging discussions.

References

Boer, G. J., N. A. McFarlane, R. Laprise, J. D. Henderson and *J.-P. Blanchet,* 1984: The Canadian Climate Centre spectral atmospheric general circulation model. Atmosphere-Ocean **22,** 397–429.

Bretherton, F. P., 1969: Momentum transport by gravity waves. Quart. J. R. Met. Soc. **95,** 213–243.

Cubasch, U., K. Hasselmann, H. Höck, E. Maier-Reimer, U. Mikolajewicz, B. D. Santer and *R. Sausen,* 1992: Time-dependent greenhouse warming computations with a coupled ocean-atmosphere model. Clim. Dyn. **8,** 55–69.

Egger, J. and *K. P. Hoinka,* 1992: Fronts and Orography. Meteorol. Atmos. Phys. **48,** 3–36.

Jaurraud, M., A. J. Simmons and *M. Kanamitsu,* 1985: Impact of an envelope orography in the ECMWF model. Proceedings of ECMWF Seminar on Physical Parameterizations, 9–13 Sep. 1985, Volume 2, 199–249.

Laursen, L. and *E. Eliasen,* 1989: On the effect of the damping mechanisms in an atmospheric general circulation model. Tellus **41A,** 385–400.

Lilly, D. K., 1972: Wave momentum flux – a GARP problem. Bull. Am. Met. Soc. **53,** 17–23.

Lilly, D. K. and *P. J. Kennedy,* 1973: Observations of a stationary mountain wave and its associated momentum flux and energy dissipation. J. Atmos. Sci. **30,** 1135–1152.

McFarlane, N. A., 1987: The effect of orographically excited gravity wave drag on the general circulation of the lower stratosphere and troposphere. J. Atmos. Sci. **44,** 1775–1800.

Miller, M. J., T. N. Palmer and *R. Swinbank,* 1989: Parametrization and influence of subgrid-scale orography in general circulation and numerical weather prediction models. Meteorol. Atmos. Phys. **40,** 84–109.

Palmer, T. N., 1987: Modelling low frequency variability of the atmosphere. Atmospheric and oceanic variability, Ed. H. Cattle, Royal Meteorological Society, 75–103.

Palmer, T. N., G. J. Shutts and *R. Swinbank,* 1986: Alleviation of a systematic westerly bias in general circulation and numerical weather prediction models through an orograhic gravity wave drag parametrization. Quart. J. R. Met. Soc. **112,** 1001–1039.

Ponater, M. and *W. König,* 1991: Interannual circulation regime fluctuations and their effect on intraseasonal variability. Meterologisches Institut der Universität Hamburg, Report No. 9, 133–162.

Rind, D., R. Suozzo, N. K. Balachandran, A. Laas and *G. Russel,* 1988: The GISS global climate – middle atmosphere model. Part I: Model structure and climatology. J. Atmos. Sci. **45,** 329–370.

Roeckner, E., K. Arpe, L. Bengtsson, S. Brinkop, L. Dümenil, M. Esch, E. Kirk, F. Lunkeit, M. Ponater, B. Rockel, R. Sausen, U. Schlese, S. Schubert and *M. Windelband,* 1992: Simulation of the present day climate with the ECHAM model: Impact of model physics and resolution. Max-Planck-Institut für Meteorologie, Report No. 93, 172 pp.

Shutts, G. J., 1985: Parametrization of sub-grid scale gravity wave momentum transfer and its influence in forecast/climate models. Proceedings of ECMWF Seminar on Physical Parametrizations, 9–13 Sep. 1985, Volume 2, 167–198.

Simmons, A. J., D. M. Burridge, M. Jarraud, C. Girard and *W. Wergen,* 1989: The ECMWF medium range prediction model, development of the numerical formulation and the impact of increased resolution. Meteorol. Atmos. Phys. **40,** 28–60.

Slingo, A. and *D. W. Pearson,* 1987: A comparison of the impact of an envelope orography and of a parametrization of orographic gravity-wave drag on model simulations. Quart. J. R. Met. Soc. **113,** 847–870.

Tibaldi, S., T. N. Palmer, C. Brankovic and *U. Cubasch,* 1990: Extended-range predictions with ECMWF models: Influence of horizontal resolution on systematic error and forecast skill. Quart. J. R. Met. Soc. **116,** 835–866.

Tibaldi, S., 1986: Envelope orography and maintenance of the quasi-stationary circulation in the ECMWF global models. Adv. in Geophys. **29,** 339–374.

Wallace, J. M., S. Tibaldi and *A. J. Simmons,* 1983: Reduction of systematic forecast errors in the ECMWF model through the introduction of an envelope orography. Quart. J. R. Met. Soc. **109,** 683–717.